ORIGINAL RESEARCH

Check for updates

Electrorheological behavior of cellulose in silicon oil. The effect of filler morphology

Victoria V. Kovaleva · Nikita M. Kuznetsov ·
Yuriy D. Zagoskin · Sergey N. Malakhov ·
Artem V. Bakirov · Sergei N. Chvalun

Abstract A comprehensive study of the cellulose particle shape effect on electrorheological activity of their suspensions in polydimethylsiloxane was performed. Microparticles, nanorods and porous composite particles of cellulose with polyethylene glycol were considered as a filler. The structure of particles was established by a set of complementary methods, such as electron microscopy, infrared spectroscopy, and wide-angle X-ray scattering. The rheological behavior of suspensions filled by various types of particles changes under an electric field. The yield stress increases with electric field strength. The role of particle shape on the electrorheological properties of suspensions was revealed. The values of the yield stress of suspensions increase from microparticles to nanorods and porous composite particles at the same concentration and electric field strength. Porous composite particles of cellulose, a novel filler obtained by freeze-drying, demonstrates an enhanced electrorheological response compared to micro- and nanoparticles. The yield stress reaches 450 Pa at 7 kV/mm at an extremely low concentration of 1.0 wt%. Moreover, the porosity of the particles significantly increases the sedimentation stability of cellulose suspensions in polydimethylsiloxane. The high porosity of the filler makes it possible to obtain highly efficient electrorheological fluids at a sufficiently low concentration of the dispersed phase.

Keywords Stimuli-responsive materials · Electrorheological fluids · Cellulose · Polyethylene glycol · Porous particles

V. V. Kovaleva · N. M. Kuznetsov (✉) · Y. D. Zagoskin ·
S. N. Malakhov · A. V. Bakirov · S. N. Chvalun
Laboratory of Polymer Materials, Nanobiomaterials and Structures Department, National Research Center "Kurchatov Institute", Pl. Academician Kurchatov, 1, 123182 Moscow, Russia
e-mail: kyz993@yandex.ru

A. V. Bakirov · S. N. Chvalun
Laboratory of Functional Polymer Structures, Enikolopov Institute of Synthetic Polymeric Materials of Russian Academy of Sciences, Profsoyuznaya Str., 70, 117393 Moscow, Russia

Introduction

A wide range of research is currently devoted to smart materials that are able to change their properties under the influence of certain external stimuli, for example, temperature or radiation, pH of the medium, electric or magnetic fields (Dong et al. 2019; Nasseri et al. 2020). Electrorheological fluids (ERFs) are special among this class of materials. They are heterogeneous systems, usually consisting of a dielectric dispersion medium and polarizable dispersed phase particles, often referred to as a filler (Kuznetsov et al. 2022a). The electrorheological (ER) effect is

reversible and controlled change of rheological properties, such as viscosity, yield stress, storage and loss moduli of the fluid by an electric field. Its nature is related to the polarization of the filler particles followed by subsequent formation of the columnar structures in the dielectric medium (See 2000; Kuznetsov et al. 2021a). The rapid and reversible response of ERF to an external electric field results in a wide range of potential applications in fast switching dampers and valves (Kolekar et al. 2019; Bauerochs et al. 2020), soft robotics (Hines et al. 2017), microfluidic chips (Sheng and Wen 2012), tactile response sensors, medicine (Chou et al. 2020; Guo et al. 2020), etc. However, despite the great achievements in the field of electrorheology, there are a number of obstacles to the widespread use of ERFs. These include typical high concentration of suspensions (more than 10 wt%) to achieve a pronounced ER effect, the high electric field strength, low sedimentation stability of ERFs, the lack of a universal description of ER mechanism, etc. One of the problems with highly concentrated fluids is their price, as the filler is often the most expensive component. Reducing the filler concentration while maintaining the performance characteristics of fluids is an urgent economic task. Therefore, modern studies are aimed to search and develop novel fluids with fillers exhibiting high ER activity at low concentrations, followed by findings of the relationship between rheological behavior and the structural and electrophysical characteristics of materials.

Low molecular weight polydimethylsiloxanes (PDMS) are widely used as the dispersion medium of ERFs. These organosilicon polymers are biocompatible and available in a wide range of viscosities, have low dielectric permittivity, chemical and thermal stability, high siloxane chain flexibility (Wolf et al. 2018). Nevertheless, the key component of ERF is the filler. According to published scientific studies, polarizable micro- and nanoparticles of various chemical nature are used as a filler: from inorganic materials (metal oxides, carbon nanomaterials and clays) (Dhar et al. 2017; Wu et al. 2018; Sokolov et al. 2021; Kuznetsov et al. 2022c) to semiconductor polymers (Lim and Choi 2017; Plachý et al. 2021) and biodegradable polysaccharide particles (Ko et al. 2011; Choi et al. 2017; Kovaleva et al. 2022b). It has been repeatedly confirmed that by varying the shape and morphology of the filler it is possible to increase the ER effect and improve the

sedimentation stability of suspensions. In particular, particles with a high aspect ratio are able to form stronger structures in an electric field resulting in a higher yield stress (Yin et al. 2009; Kovaleva et al. 2022b). In turn nanosized filler can improve the sedimentation stability of ERFs (Yin et al. 2009).

Polymeric materials, due to their variability, open up a range of possibilities for producing ERF fillers (He et al. 2022). Among polymer particles, the porous ones are another promising filler. If the pore size is large enough, the molecules of the dispersion medium can penetrate into the porous structure of particles. Thus, a percolation network from particles is formed in the suspension at a low concentration (less than 5 wt%) resulting in enhanced sedimentation stability of suspensions. The percolation network is reinforced in an electric field leading to an increased ER effect. Thus, the high ER activity of porous chitosan particles in PDMS and olive oil was recently shown (Kuznetsov et al. 2021c, d). Suspensions in PDMS proved to be stable in a wide range of electric field strengths up to 7 kV/mm. The equilibrium sedimentation ratio for 1.0 wt% ERF is more than 90% and the yield stress reaches 540 Pa (Kuznetsov et al. 2021d). It should be noted that suspensions exhibit a stable response in a wide temperature range (Kovaleva et al. 2022a), and additionally, the introduction of nanoparticles into the porous structure opens up opportunities for directed regulation of the ER activity of the filler over a wide range (Kuznetsov et al. 2021b, 2022b). Moreover, low filler concentration can also reduce the costs of the material. Therefore, the porous particles are of great interest.

According to green chemistry paradigm, the biocompatible and biodegradable fillers are encouraged to produce environmentally friendly materials. In this vein, polysaccharide fillers are extremely promising. Thus, cellulose, starch, chitin, and chitosan can polarize due to the lateral polar groups and exhibit the ER effect. Cellulose is the most abundant biopolymer on the planet. It is a linear polysaccharide with D-glucose monomers, which are linked through β-(1→4) bonds. In nature cellulose consists of amorphous and crystalline regions. Depending on the feedstock and isolation methods, cellulose can be obtained as wood fiber, microfibrils, micro- or nanocrystals, etc., differing in morphology, length, aspect ratio, and degree of crystallinity (Choi et al. 2017).

The ER activity of cellulose and its composites has been demonstrated previously. Thus, ERFs filled by microcrystals and microfibrils of cellulose in silicone oil have been reported (Sim et al. 2016; Choi et al. 2019). The yield stress values were achieved up to several hundred Pa at low field strength (1–2 kV/mm) and a concentration of 10 wt%. The yield stress values were directly proportional to the cellulose weight fraction, which the authors attribute to a corresponding increase in the number of chains in the colloid structure. It has been recently demonstrated that cellulose nanofibrils and nanocrystals also reveal ER activity in castor oil at low concentrations (less than 6 wt%) (García-Morales et al. 2020). It was found that the shape of the particles affects the ER properties, the yield stress of suspension was higher for nanofibrils. In particular, the yield stress reaches about 300 and 375 Pa at 4 kV/mm and 4 wt% for cellulose nanocrystals and nanofibrils, respectively. However, the morphology of filler particles was not confirmed. Derivatives and composite cellulose particles are also being actively explored as ERF fillers. It was reported on the use of phosphate (Bae et al. 2017) and lithium carboxyl salt (Tilki et al. 2010) of cellulose, hydroxypropyl cellulose (Misono and Negita 2004), surface modified cellulose (Liu et al. 2018), and various composites of this polysaccharide (Kraev et al. 2007). Nevertheless, despite the wide utilization of various types of cellulose and its composites in electrorheology, porous cellulose particles have not previously been used as filler for ERFs. However, porous cellulose and its derivatives have already been obtained by various methods, including the preparation of highly porous microspheres by dissolving particles of TEMPO-oxidized cellulose in NaOH/urea solution, followed by dispersion in paraffin oil and emulsification (Zhang et al. 2022), and the preparation of porous composite films from cellulose acetate with sodium nitrate (Lee et al. 2022). Thus, despite the rather high number of studies devoted to ERFs with cellulose, a direct comparison of the particle shape and morphology effect on the ER behavior of low-concentrated suspensions in PDMS has not been performed. That is why the aim of this research is to study the role of cellulose particles morphology on the ER effect and to improve the ER properties of cellulose suspensions by obtaining porous particles.

Material and methods

Silicon oil (PDMS) (PMS-100, Penta-Junior LLC, Russia) with the kinematic viscosity of 100 cSt was used as a dispersion medium. Previously, the oil was characterized by size-exclusion chromatography and rotational viscometry. The average molecular weight M_w is 12.2 kDa, the polydispersity index is 2.0 and the viscosity is 105 mPa·s (Kuznetsov et al. 2021d). Three types of cellulose particles were used as filler, namely microparticles (MC, Sigma Aldrich, Ireland), nanorods (NC, CNF, Nanografi Nanotechnology AS, Germany) and porous composite particles of cellulose with polyethylene glycol (PEG, 35 kDa, Sigma Aldrich, Germany) as a binder. Commercial NC powder was pre-dispersed in water at a concentration of 0.5 wt%. In the first step, the 0.5 wt% suspension was stirred on an MR Hei-Tec magnetic stirrer (Heidolph, Germany) at 350 rpm for 24 h. The sample was then subjected to ultrasonication for 20 min in a UZV-4.0/1 TTTs (RMD) bath (150 W, 35 kHz, LLC Sapphire, Russia) and freeze-dried on the device Alpha 1–2 LDPlus (Martin Christ, Germany) for 3 days under vacuum 0.250 mbar, followed by drying at 0.030 mbar for 5 h before preparing suspensions in PDMS to obtain more reliable results utilizing the NC as a filler.

Porous cellulose particle fabrication

Porous particles were produced by the procedure similar to previously described for chitosan (Kuznetsov et al. 2021d). Cellulose does not dissolve in most common solvents, due to its supramolecular organization and high crystallinity. Therefore, a PEG binder was used to obtain highly porous particles by freeze-drying. At the first stage, suspensions of NC in aqueous solution of PEG were prepared. The ratio of NC to PEG was varied, so the composite particles contain 1, 5, 10 and 50 wt% of the polymeric binder. The total concentration of NC and PEG in solution was 1 wt%. The suspensions were pneumatically sprayed into a bath with liquid nitrogen forming freezed drops. After that, the particles were kept in the refrigerator at -24 °C to completely evaporate nitrogen. The obtained samples were freeze-dried using Alpha 2–4 LDPlus (Martin Christ, Germany) for 3 days at a condenser temperature -74 °C under a vacuum of 0.250 mbar with following final drying at 0.030 mbar

for 5 h. Porous particles from PEG were also fabricated as reference. Thus, composite highly porous cellulose particles with different content of the binder were isolated, hereinafter denoted as C/1%PEG, C/5%PEG, C/10%PEG, C/50%PEG, PEG depending on PEG content.

ERFs preparation

ERFs with 1.0 wt% filler content were prepared by dispersing a selected particle type in PDMS for 72 h on an MR Hei-Tec magnetic stirrer (Heidolph, Germany) at 350 rpm. Additionally, ultrasonic treatment was performed for 20 min in a UZV-4.0/1 TTTs (RMD) bath (150 W, 35 kHz, LLC Sapphire, Russia) before each measurement.

Electron microscopy

The morphology of MC and NC particles was studied by scanning electron microscopy (SEM) via a Versa 3D microscope (ThermoFisher Scientific, USA) in a high vacuum mode. The signal was detected from secondary electrons with an ETD detector (ThermoFisher Scientific, USA). Accelerating voltage and current were set up to 2 kV and 33 pA, respectively. A thin layer of gold was applied to the sample surface before measurements were done to minimize the accumulation of electric charge. The morphology of porous particles was performed using a Phenom XL microscope (ThermoFisher Scientific, USA) equipped with backscattered and secondary electron detectors at pressure of 0.1 Pa and accelerating voltage of 5 kV. Additionally, suspension of 0.1 wt% NC in water was studied by transmission electron microscopy (TEM). The measurements were performed via a Titan 80–300 microscope (ThermoFisher Scientific, USA) at accelerating voltage of 300 kV. Samples for TEM studies were prepared using negative staining. At the first stage, the surface of copper grids with a Pelco Pure C carbon substrate (Ted Pella Inc., USA) was hydrophilized using glow discharge treatment in a Pelco EasiGlow setup (Ted Pella Inc., USA) for 30 s at a current of 25 mA and pressure of 0.26 mbar. Next, a negative staining procedure was performed using 1.0 wt% uranyl acetate solution (Ted Pella Inc., USA) according with to the well-known protocol

(Hajibagheri 1999). Particle size distribution diagrams were calculated manually using ImageJ software. At least 100 particles were used during data processing.

Optical microscopy

To qualitatively study the dispersion of commercial and freeze-dried cellulose in water and PDMS further characterization of suspensions by optical microscopy was performed using the Carl Zeiss Axio Imager. M2m microscope. Measurements were performed in two modes: with and without crossed polarizers. Substances were placed between glass coverslips. A 5×magnification objective was used. Image processing was performed in the Axio Vision program.

Infrared spectroscopy

The chemical structure of the cellulose filler particles of various morphologies was confirmed by infrared (IR) spectroscopy. The measurements were performed on a Nicolet iS5 IR Fourier Transform spectrometer (Thermo Fisher Scientific, USA) with an iD5 ATR accessory with a diamond crystal. IR spectra were measured in the range of 500–4000 cm^{-1} with a resolution of 4 cm^{-1}.

Wide-angle X-ray scattering

The structure of the fillers was studied by wide-angle X-ray scattering (WAXS) at BioMur beamline of Kurchatov synchrotron radiation source (Russia). The used wavelength was $\lambda = 1.445$ Å, 2D detector Dectris Pilatus 1 M was used. The powders of MC and NC were measured in X-ray capillaries (Hilgenberg, Germany) with wall thickness of 10 μm and diameter of 1.5 mm, while porous particles were placed between two Kapton rollers fixed by an annular holder. The sample-detector distance was calibrated using silver behenate ($d_{001} = 58.38$ Å). The distance between the measuring cell and the detector was 150 mm. The exposure time depended on the scattering intensity of the sample and was varied for filler powders from 10 to 300 s. Primary processing of 2D images was performed using the Fit2D program (ESRF, France). The crystallinity degree of the studied samples was calculated by the following equation (Park et al. 2010):

crystallinity degree CD (%) = $100 \times$ Sc / St, where Sc represents the area of the crystalline domains and St the area of the total domains, respectively.

Rheological tests

Rheological measurements were performed via a rotational rheometer Physica MCR 501 (Anton Paar, Germany) with the geometry of concentric cylinders, measuring cell CC-27E (ISO 3219). All measurements were performed with an electrorheological setup (Anton Paar, Germany) without any additional modifications. A constant electric field up to 7 kV/mm was applied from an external source FuG HCP 14—12500 MOD (FuG Elektronik GmbH, Germany). The gap between the cylinders was 1 mm, and the cell volume was 20 ml. The measurements were performed in the controlled shear stress (CSS) mode to determine the static yield stress. The shear stress was varied from 0.1 to 100 or 500 Pa depending on the sample and the electric field strength. The measurement time was changed according to a logarithmic law from 10 to 5 s per point for 100 points range. The test was performed with a sequential increase in shear stress. The yield stress was determined from the typical sharp break in the flow curve in linear coordinates. The flow and viscosity curves were defined in the controlled shear rate (CSR) mode. The measurements were performed with a sequential increase of the shear rate from 0.01 (for measurements without an electric field) and from 0.1 (under an electric field) up to 1000 s^{-1}. The range was 10 points per decade, with the measurement time per point changing from 100 to 1 s according to the logarithmic law. Frequency sweeps of the storage and loss moduli were obtained at the low deformation amplitude (0.1%) in the linear range of visco-elasticity. The measurements were performed by decreasing the frequency from 500 to 0.1 rad/s in an automatic mode. The data were processed using the Rheoplus 3.40 software package and the Origin software.

Sedimentation stability

Sedimentation stability of suspensions was evaluated for 3 weeks at room temperature by the sedimentation ratio. It is the ratio of the colloidal phase height to the entire fluid height.

Results and discussion

Fillers morphology

Typical micrographs of different types of cellulose particles are shown in Fig. 1. Surprisingly, micron-sized particles are observed in the SEM images for both the MC and NC powders (Fig. 1a, b). One can see a higher aspect ratio of "microfibrils" of the NC sample and their smoother surface compared to MC. However, macrofibers are destroyed to individual nanocrystals when NC powder is dispersed in water (Fig. S1a,b) in contrast to MC sample that retains its morphology. That is why, freeze-dried NC particles from an aqueous dispersion were used as a filler. TEM images demonstrate highly anisometric nanoparticles with dimensions of 100 ± 20 nm in length and 6 ± 1 nm in diameter, with an aspect ratio of 16 ± 2 (Fig. 1c). Calculated aspect ratio is about 5 times higher than that for the MC sample with the average diameter, length and aspect ratio of 11 ± 4 μm, 34 ± 12 μm and 3 ± 1, respectively (Fig. S2). It is worth noting that commercial CNFs retain the morphology of macrofibrils in PDMS. However, freeze-dried NC particles, are not completely transformed into nanocrystals when dispersed in PDMS as well. According to optical microscopy, a single aggregates of micron-sized particles are observed in the suspension in contrast to directly mixing the commercial CNF with PDMS (Fig. S1c,d). Unfortunately, an accurate quantitative estimation of the nanoparticles and residual microfibrils fraction in the dispersion is complicated. The related experimental difficulties are discussed in the appropriate section of Supplementary Information. Thus we assume that the majority of the freeze-dried NC particles in PDMS are nanocrystals.

Porous particles have a mainly spherical morphology with open pores of various sizes regardless of composition. Figure 1d shows C/1%PEG particles as an example. The size of particles is on micron scale, the pore size reaches several microns, forming a structure of penetrating channels. The porosity of the particles is higher than 90%. Images for porous particles of other compositions are presented in Fig. S3. The particle diameter distribution diagrams show quite a wide distribution (Fig. S4), due to the viscosity variation of solution during the spraying

Fig. 1 SEM micrographs of MC (**a**), NC (**b**) and C/1%PEG porous particles (**d**) powders. Typical TEM image of a 0.1 wt% aqueous solution of NC (**c**)
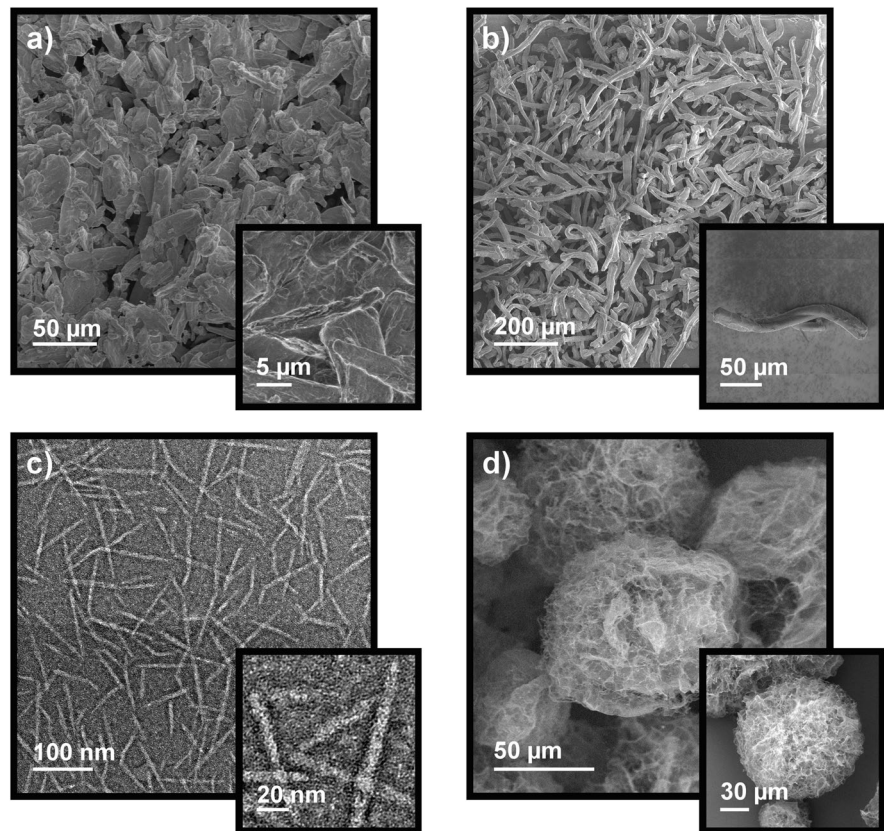
process of filler fabrication (Kuznetsov et al. 2022b). The most expected value of diameters for C/1%PEG, C/5%PEG, C/10%PEG, C/50%PEG are 70, 100, 100, and 150 μm, respectively.

Chemical structure of fillers

All fillers were characterized by IR spectroscopy, the corresponding spectra are shown in Fig. 2a, b. A strong broad band in the region of 3600–3000 cm^{-1} is assigned to stretching vibrations of hydrogen-bonded O–H groups. Three types of hydrogen bonds can be distinguished in the cellulose structure, two are intramolecular (3OH···O5, 3336 cm^{-1} and 2OH···O6, shoulder at ~3500 cm^{-1}) and one is intermolecular (6OH···O3′, shoulder at ~3200 cm^{-1}) (Cichosz and Masek 2020). The maximum at 3336 cm^{-1} designates that intramolecular hydrogen bonds are more pronounced. The absorption maximum at 2900 cm^{-1} corresponds to stretching vibrations of the C–H group. An intense band with a maximum at about 1640 cm^{-1} belongs to the bending vibrations of the O-H groups

of adsorbed water (Kassab et al. 2020). The peaks observed in the region of 1429–1316 cm^{-1} and 1056 cm^{-1} correspond to bending vibrations of the C–H bond (Chen et al. 2016). The bands in the region from 800 to 1200 cm^{-1} are attributed to stretching vibrations of C–O, C–C and ring structures, as well as to external bending vibrations of CH$_2$, COH, CCO, CCH groups. The band of stretching vibrations at ~900 cm^{-1} in the spectrum of cellulose indicates an asymmetric vibration of the ring in antiphase and vibration of the C^1 atom and four surrounding atoms in the spectra of β-glycoside structures (Zhao et al. 2017; Kassab et al. 2020). The absorption maximum at 1595 cm^{-1} for the NC sample can be associated with the stretching vibrations of the aromatic C=C bond (Wu et al. 2019; Melikoğlu et al. 2019) or may be caused by the presence of C=O stretching vibration of carboxyl group (Kassab et al. 2020).

The IR spectra of composite cellulose particles with PEG as well as individual components are presented in Fig. 2b. Absorption bands at 2920 and 2885 cm^{-1} belong to the PEG alkyl chain, and the
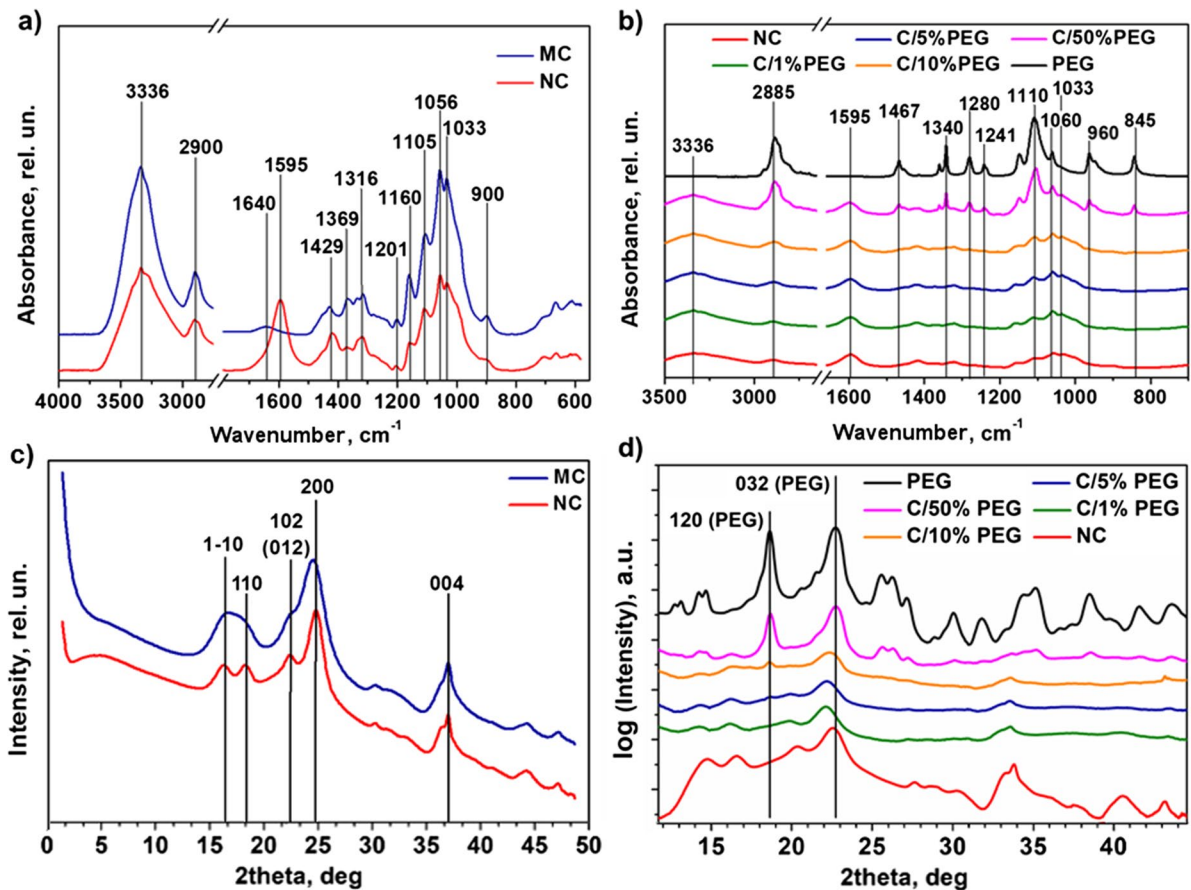
Fig. 2 IR-spectra (**a**, **b**) and WAXS curves (**c**, **d**) for the MC and NC powders (**a**, **c**) and porous particle powders C/PEG of different composition and pure PEG (**b**, **d**). The curves are shifted along the y-axis for clarity

peaks in the ranges of 1480 and 1200 cm^{-1} correspond to the C–H bending vibrations and the C–O–C stretching vibration of the ether group, respectively (León et al. 2017). The intensity of PEG characteristic peaks increases with concentration in the particles, as was expected. It should be noted that C–O–C stretching peaks of PEG overlap with the absorption bands of cellulose. Thus, one can assume an increase in the concentration of PEG in the composition of particles by an increase in intensity of C–H bending bands.

WAXS studies allow confirming the nature of fillers and evaluating the crystallinity degree (Fig. 2c, d). Cellulose is known to exist in several polymorphic modifications (I–IV), which are able to transform into each other (French 2014). Cellulose I is present in a large number of organisms, with I_α occurring in algae and bacteria, and I_β being more common in plants

(Jin et al. 2016). Both modifications of cellulose differ in the type of symmetry. Cellulose fillers used in the study have high crystallinity and are in I_β modification according to WAXS data. The specific patterns are marked in Fig. 2c. Raw integrated scattering data without and with absorption correction are provided in Fig. S5a,b. The degree of crystallinity and coherent scattering length in different directions of the crystal are presented in Table 1, apparent peak deconvolution is shown in Fig. S5c,d.

Porous cellulose particles with PEG content of 1, 5 and 10% show several weak crystalline reflections compared to C/50%PEG sample and pure PEG (Fig. 2d). Since the d-spacings of the most intense reflections of (032) PEG and (200) of cellulose I_β are close, one can differ the dominating crystal phase judging the intensity of (120) PEG and (004) NC reflections. All particles with PEG content below

Table 1 The results of WAXS data processing

Sample	Degree of crystallinity, %	Coherent-scattering length, nm				
		(1–10)	(110)	(102)	(200)	(004)
NC	49.4	6.1	4.6	10.6	7.1	9.8
MC	56.6	5.5	3.4	4.7	5.1	10.0
PEG	78.0		**(120)**		**(032)**[a]	
			16.5		10.1	

ᵃOverlap of (032), ($\bar{1}$32), (112), ($\bar{2}$12), ($\bar{1}$24), ($\bar{2}$04), and (004) reflections

10% show no distinct (120) PEG peak, thus showing prevaling crystalline phase of cellulose. The particles with 10% of PEG reveal both PEG and cellulose reflections, while exceeding this value retains only PEG reflections, but with low overall degree of crystallinity.

Thus, the pure porous PEG particles have high degree of crystallinity. The observed features can be explained by two factors. PEG is known to be able to crystallize (He and Xu 2012; Golitsyn et al. 2019), and moreover show special crystal orientation in confined conditions (Yarysheva et al. 2017). Therefore, when a solution is sprayed into liquid nitrogen, during the formation of particles, the solvent crystallizes and the polymer chains segregate into the particle walls. In the absence of NC in the matrix solution, PEG chains are packed and the walls of particles are crystalline. The presence of NC in the suspension during the preparation of composite particles sterically hinders the stacking of PEG chains leading to crystallization hindering. The low intensity of crystalline reflections of NC in the scattering curves can be explained by the low density of the material and the masking of scattering by the amorphous material. Nevertheless, it was able to detect both crystal lattices simultaneously during the phase separation inside particles. The degree of crystallinity and the length of coherent scattering were determined for porous particles made of pure PEG as well (Table 1).

Rheological behavior of cellulose suspensions

The suspensions with 1.0 wt% of various types of cellulose particles in PDMS were prepared to study their ER properties. Flow and viscosity curves for pure PDMS and suspensions of MC, NC, and C/1% PEG particles are shown in Fig. 3. PDMS behaves like a Newtonian fluid and its viscosity does not depend on the shear rate (Fig. 3b) (Malkin and Isayev 2005). When cellulose is added to PDMS, its rheological behavior changes. The viscosity of suspensions increases regardless of the filler type. Such effect is especially noticeable at low shear rates. It should be noted that a more significant increase in viscosity and the yield stress are observed on the flow curve for the C/1%PEG sample compared to MC and NC suspensions (Fig. 3a). Special attention should be paid to the flow and viscosity curves of the C/1%PEG sample. There is a dip at 3 s⁻¹ in the dependences. The obtained data can be attributed to various factors, including the slip effect, concentration gradient near the wall typical for any dispersion, particle structural rearrangement, and filler morphological features. The reason for such unusual rheological behavior is beyond the scope of presented manuscript, however short discussion of this issue is presented in Supplementary Information, Fig. S6. The rheological behavior of suspensions filled by porous particles of a different composition is quite similar to the dependence shown in Fig. 3 for C/1%PEG sample. Thus, all studied suspensions reveal weak elastic response followed by the formation of a percolation network in the suspension of porous particles.

Preliminary tests of the shear stress dependences on time with an incremental change in the electric field strength and a shear rate of 0.1 s⁻¹ were provided to identify the ER activity of composite particles with PEG and evaluate the effect of the composition on the ER properties (Fig. S7a). Suspensions of porous PEG particles do not exhibit the ER effect. The shear stress of suspensions is unchanged under an electric field. The ER response of suspensions appears and increases with an increase in the cellulose concentration in the particles, and shear stress reaches a maximum at a minimum PEG content (1 wt%). Therefore, further measurements were performed for the C/1%PEG particles suspension, because it is of the most interest.

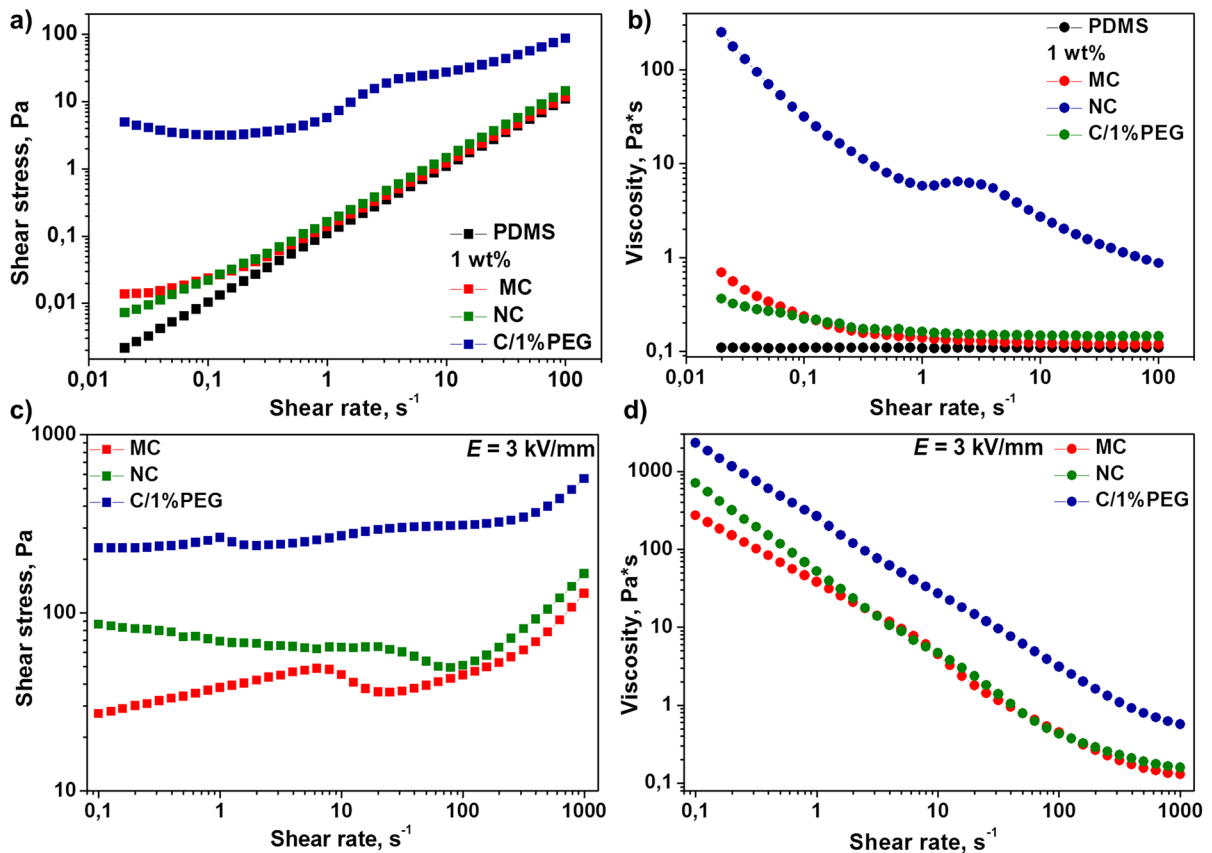The electric field dramatically affects the rheological behavior of cellulose suspensions. Figure 3c,

Fig. 3 Flow (**a**, **c**) and viscosity (**b**, **d**) curves of 1.0 wt% ERFs filled with MC, NC, and C/1% PEG particles at electric field of 0 kV/mm (**a**, **b**) and 3 kV/mm (**c**, **d**). The measurements were performed in the CSR mode

d shows the flow and viscosity curves of the studied suspensions at electric field strength of 3 kV/mm as an example. The corresponding flow curves of the samples at other electric field strengths are shown in Fig. S8. For all samples, the yield stress appears on the flow curves and their values increase with electric field strength (Fig. 3c, Fig. S8a, c, e). The viscosity curves show a corresponding increase in values when an electric field is applied. Moreover, the viscosity of the suspensions also increases with an electric field strength (Fig. S8), Thus, suspensions exhibit the pronounced ER effect. The dependencies indicate the formation and strengthening of the percolation network in the suspensions. The decrease in viscosity with shear rate is typically explained by the destruction of the columnar structures formed by the particles.

The differences in the ER behavior of suspensions are more clearly demonstrated by the dependence of the static yield stress on the electric field strength. A significant increase in the values is observed with an electric field for all the samples (Fig. 4a). The maximum yield stress of 450 Pa at 7 kV/mm was achieved for 1.0 wt% suspension of C/1%PEG particles. Typically, the value of the yield stress is directly proportional to the electric field strength in the power law of $1 \leq k \leq 2$ (Kuznetsov et al. 2022a). Based on the value of exponent k, one can draw a conclusion about the effect of conductivity and polarization on the mechanism of the ER effect. If polarization is the main factor, then k is close to 2. The significant contribution of conductivity in the ER effect leads to a decrease of the exponent down to 1.5, and k is close to 1 when the polarization is saturated (Seo et al. 2017). It can be seen that the slope of the dependencies (exponent k) depends on the cellulose particle type (Fig. 4a). Thus, the values of the yield stress of 1.0 wt% suspensions proportional to 1.8, 1.5 and 1.2 for MC,
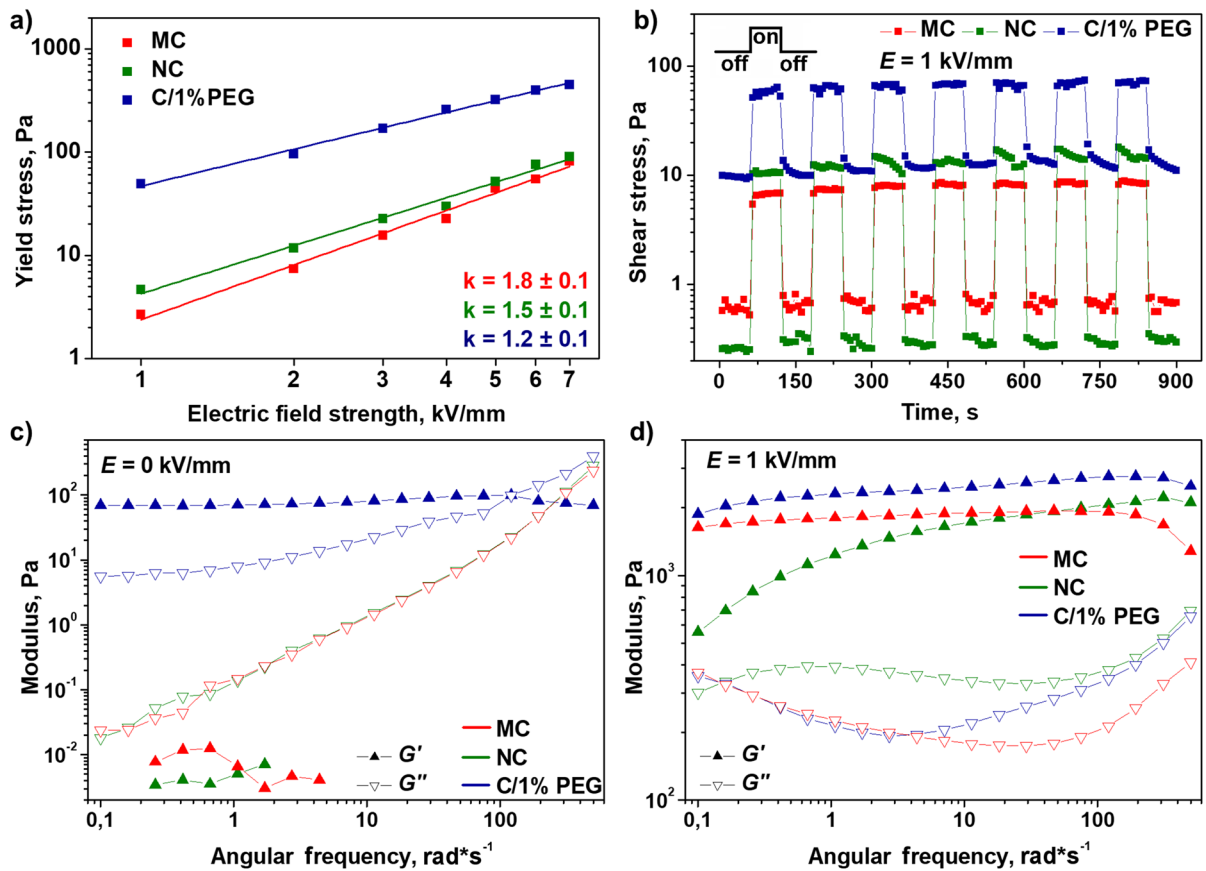
Fig. 4 Yield stress as a function of electric field strength for 1.0 wt% suspensions of cellulose particles of various morphologies in PDMS in double logarithmic scale (**a**). Measurements were performed in CSS mode. Shear stress as a function of time under switching an electric field of various cellulose suspensions (**b**). The measurements were performed in the CSR mode at a shear rate of 1 s^{-1} and electric field strength of 1 kV/mm. Frequency dependences of storage (G') and loss (G'') moduli of the samples at electric field of 0 kV/mm (**c**) and 1 kV/mm (**d**)

NC and C/1%PEG suspensions. An exponent value of ~1.5 has been previously reported for various ERF fillers, including chitin, chitosan, and cellulose composites (Yoon and Kim 2006; Kuznetsov et al. 2021b, d; Kovaleva et al. 2022b). It is interesting to note that the mechanism of the ER effect of MC suspensions in the olive oil medium is more complex and reveals a transition from polarization to saturated polarization mechanism at a critical electric field of 3 kV/mm (Kuznetsov et al. 2023). The exponent decreases down to 1.2 for ERF filled by C/1%PEG particles. There are several possible reasons for such behavior, for example hydrogen bonds including interactions of the filler with the dispersion medium (Spence et al. 2010; Bogdanova et al. 2016) or polarization saturation (Huang et al.

2006). Thus, the mechanism of the ER effect is more complex.

The stability of the ER response is of great importance for practical applications. Therefore, the obtained ERFs were studied in the on/off mode of an electric field. The time dependence of the shear stress during electric field switching for the studied suspensions of cellulose at electric field strength of 1 kV/mm are shown on Fig. 4b. The shear stress rapidly increases under an electric field, indicating the formation of columnar structures in the suspension. A continuous decrease in shear stress values after turning off the electric field is most likely due to the relaxation of the structure. Finally, the shear stress is almost reduced to its original value. It should be noted that the degradation of shear stress values with

Table 2 Relative efficiency of 1.0 wt% ERFs

Electric field, kV/mm	MC		NC		C/1%PEG	
	Ef_{rel}, rel. un.	K_{eff}, rel. un.	Ef_{rel}, rel. un.	K_{eff}, rel. un.	Ef_{rel}, rel. un.	K_{eff}, rel. un.
1	26	2600	45	4500	15	1500
2	73	3600	120	5800	29	1500
3	150	5200	220	7500	53	1800
4	220	5600	300	7400	82	2000
5	440	8900	510	10300	100	2000
6	540	9100	760	12600	130	2100
7	810	11600	900	12800	140	2000

the number of cycles is observed for the NC sample, which is more noticeable at a strength of 4 kV/mm (Fig. S7b). Such dependence can be related to the formation of an equilibrium structure by particles, as well as with their aggregation and further formation of columnar structures from the resulting aggregates instead of individual particles. Nevertheless, all suspensions showed sufficient reproducibility of rheological properties under cyclic exposure to an electric field of various strengths. Thus, suspensions can be considered for further practical applications.

More detailed information about the balance between elastic and viscous components in suspension behavior can be provided by oscillatory rheological tests. The frequency dependences of the storage and loss moduli were determined for the studied ERFs to confirm the elastic behavior of the suspensions and the appearance of the yield stress under an electric field (Fig. 4c, d). The loss modulus increases

with angular frequency for all studied samples without an electric field (Fig. 4c). The storage modulus values are lower than those of loss modulus for MC and NC suspensions indicating the viscous behavior of the samples and confirming no yield stress of suspensions (compare with Fig. 3a). However, the storage modulus is practically independent on frequency in studied range and exceeds the loss one for the ERF filled by porous C/1%PEG particles. Such dependence confirms the percolation network formation in the suspension and also indicates the predominance of the elastic component in the rheological behavior of the sample.

The storage modulus exceeds the loss modulus for all ERFs under study in the entire frequency range under an electric field (Fig. 4d). The values of storage modulus for MC and C/1% PEG suspensions weakly depend on frequency, but increase for NC suspension. Such dependence confirms the
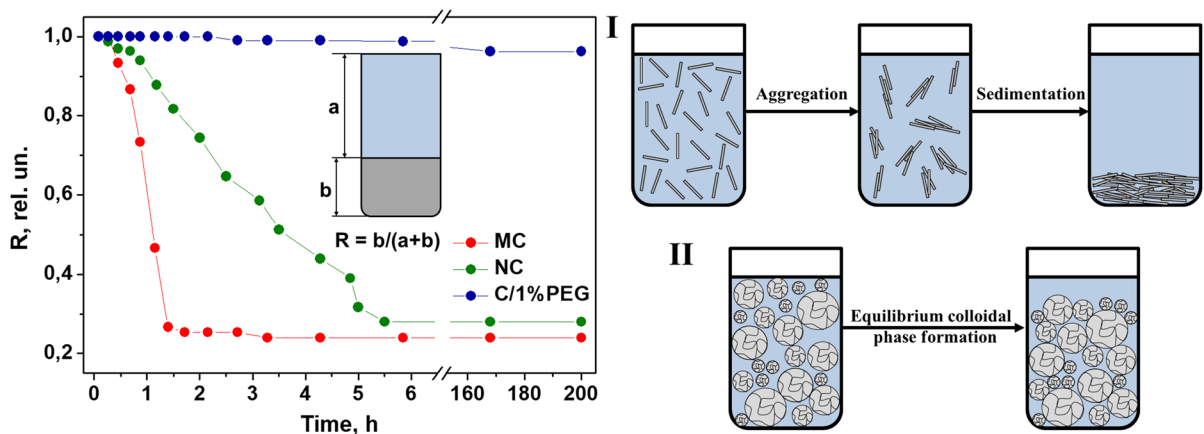

Fig. 5 The sedimentation ratio (R) dependences of ERFs filled with different types of cellulose particles. Scheme of the sedimentation process for MC and NC particles (I) and porous filler particles (II)

increase in elastic response of the suspension and the yield stress indicated by the flow curves. Thus, the elastic component predominates in cellulose suspensions, when an electric field is applied, and a strong ER effect is observed, which is more pronounced for composite cellulose particles.

The efficiency of ERFs can be assessed by the magnitude of the change in yield stress using the following equation (Jang et al. 2019):

$$Ef_{rel} = \frac{\tau_E - \tau_0}{\tau_0},$$

where τ_0 is the yield stress of fluid, τ_E is the yield stress of fluid at a given electric field strength.

The equation does not take into account the concentration of the dispersed phase and the electric field strength. Therefore, it does not allow a correct comparison of the fluids efficiency with different compositions. For this reason, an equation has previously been proposed that takes these parameters into account (Kuznetsov et al. 2022a):

$$K_{eff} = \frac{\tau_E - \tau_0}{\tau_0 E_{rel} \omega_p},$$

where E_{rel} is the normalized electric field strength, rel. un.; ω_p is the filler fraction, rel. un.

Such assessment reveals the contrast of changes in the rheological response of fluids under an electric field (Table 2). For MC and NC fluids without yield stress, a shear stress value of $\tau_0 = 0.1$ Pa was used for the calculations. It can be seen, that the most pronounced change in rheological behavior is observed for the NC suspension.

Sedimentation stability of cellulose suspensions

An important characteristic of liquid disperse systems is sedimentation stability. Figure 5 shows the dependences of the sedimentation ratio (R) on time. The stability of MC and NC suspensions turned out to be qualitatively the same and low. The equilibrium sedimentation ratio is ~25% regardless of the filler type. However, the suspension of NC particles reaches an equilibrium ratio for a longer period of ~5 h than for MC particles (2 h). The observed results indicate better aggregation stability of nanosized particles, but poor compatibility of both MC and NC particles with PDMS and their aggregation followed

by sedimentation. Nevertheless, the suspension of porous particles demonstrates improved sedimentation stability. The sedimentation ratio is more than 95%. The observed extremely high sedimentation stability of porous particles was explained earlier and is associated with the formation of an equilibrium colloidal phase due to the penetration of the dispersion medium molecules into the particles pores (Kuznetsov et al. 2021d). The differences in the sedimentation process of various types of cellulose particles are schematically shown in the Fig. 5. Thus, the porosity of the particles improves the sedimentation stability of ERF in several orders of magnitude and opens up possibilities for the long-term use of such fluids.

Conclusions

The morphology and chemical structure of cellulose particles strongly affect the ER behavior of low-filled fluids in PDMS. Based on the previously proposed approach, a novel highly effective filler was developed, namely, porous composite particles of cellulose with PEG as a binder. It was shown that only 1.0 wt% of the binder is enough to obtain and maintain the shape of highly porous particles. The morphology of cellulose has a significant effect on the ER response and sedimentation stability of suspensions. The yield stress values of fluids under electric field increase from microparticles to nanorods and to highly porous composite particles. Thus, nanorods with a higher aspect ratio than microparticles exhibit higher ER activity. However, the greatest ER effect in terms of the yield stress was obtained for ERF filled with porous particles. The yield stress of suspension reaches 450 Pa at 7 kV/mm and only 1.0 wt% of filler. This value is extremely high for such a low filler concentration. Meanwhile, the NC suspension shows the most pronounced change in rheological behavior under electric field. All the studied ERFs showed a stable response under switching electric field and can be used for practical applications. MC and NC have poor sedimentation stability in PDMS, the equilibrium sedimentation ratio of suspensions was ~25%, regardless of the particle type. The high porosity of the particles made it possible to increase the sedimentation stability of suspensions. After 3 weeks of the experiment, the sedimentation ratio remained at a high level of about 95% due to the long-term

formation of an equilibrium colloidal phase. Thus, the porosity of the particles makes it possible to improve the operational characteristics of the ERF, namely, to reduce the concentration of suspensions, to increase the ER response and the sedimentation stability of the obtained materials.

Author contributions V.K.: Investigation, Validation, Writing – original draft. N.K.: Conceptualization, Investigation, Writing – original draft. Y.Z.: Investigation, Resources. S.M.: Investigation, Writing – review & editing. A.B.: Investigation, Writing – review & editing. S.C: Conceptualization, Writing – review & editing, Supervision.

Data availability Data are available upon request.

Declarations

Competing interests The authors declare no competing interests.

Ethics approval and consent to participate Not applicable.

Consent for publication All authors give the consent to the publication of the data in the *Cellulose* journal.

References

Bae DH, Choi HJ, Choi K et al (2017) Fabrication of phosphate microcrystalline rice husk based cellulose particles and their electrorheological response. Carbohydr Polym 165:247–254. https://doi.org/10.1016/j.carbpol.2017.02.037

Bauerochs T, Huo X, Yossifon G et al (2020) Alternating current response and visualization of electrorheological fluid. J Intell Mater Syst Struct 31:288–296. https://doi.org/10.1177/1045389X19888789

Bogdanova OI, Polyakov DK, Streltsov DR et al (2016) Structure of β-chitin from Berryteuthis magister and its transformation during whisker preparation and polymerization filling. Carbohydr Polym 137:678–684. https://doi.org/10.1016/j.carbpol.2015.11.027

Chen YW, Lee HV, Juan JC, Phang S-M (2016) Production of new cellulose nanomaterial from red algae marine biomass Gelidium elegans. Carbohydr Polym 151:1210–1219. https://doi.org/10.1016/j.carbpol.2016.06.083

Choi K, Gao CY, Do NJ, Choi HJ (2017) Cellulose-based smart fluids under applied electric fields. Materials (Basel) 10:1060–1081. https://doi.org/10.3390/ma10091060

Choi K, Nam J Do, Kwon SH, et al (2019) Microfibrillated cellulose suspension and its electrorheology. Polymers (Basel) 11:2119(11). https://doi.org/10.3390/polym11122119

Chou PC, Lin FP, Hsu HL et al (2020) Electrorheological sensor encapsulating microsphere media for plague diagnosis with rapid visualization. ACS Sensors 5:665–673. https://doi.org/10.1021/acssensors.9b01529

Cichosz S, Masek A (2020) IR Study on cellulose with the varied moisture contents: insight into the supramolecular structure. Materials (Basel) 13:4573. https://doi.org/10.3390/ma13204573

Dhar P, Katiyar A, Pattamatta A, Das SK (2017) Large electrorheological phenomena in graphene nano-gels. Nanotechnology 28:035702 (12). https://doi.org/10.1088/1361-6528/28/3/035702

Dong YZ, Seo Y, Choi HJ (2019) Recent development of electro-responsive smart electrorheological fluids. Soft Matter 15:3473–3486. https://doi.org/10.1039/c9sm00210c

French AD (2014) Idealized powder diffraction patterns for cellulose polymorphs. Cellulose 21:885–896. https://doi.org/10.1007/s10570-013-0030-4

García-Morales M, Fernández-Silva SD, Roman C et al (2020) Preliminary insights into electro-sensitive ecolubricants: a comparative analysis based on nanocelluloses and nanosilicates in castor oil. Processes 8:1060(8). https://doi.org/10.3390/pr8091060

Golitsyn Y, Pulst M, Samiullah MH et al (2019) Crystallization in PEG networks: the importance of network topology and chain tilt in crystals. Polymer (Guildf) 165:72–82. https://doi.org/10.1016/j.polymer.2019.01.018

Guo JW, Lin FP, Chang CJ et al (2020) Sandwich-structured displays encapsulating polystyrene microspheres coated with Fe_3O_4 nanoparticles for label-free biosensing for electrorheological operation. Sensors Actuators B Chem 302(13):127185

Hajibagheri MAN (1999) Electron microscopy methods and protocols. Humana Press Inc., Totowa, New Jersey. https://doi.org/10.1385/1592592015

He WN, Xu JT (2012) Crystallization assisted self-assembly of semicrystalline block copolymers. Prog Polym Sci 37:1350–1400. https://doi.org/10.1016/j.progpolymsci.2012.05.002

He F, Lei Q, Zhao X, Yin J (2022) Polyelectrolyte-based electrorheological materials. Polymer (Guildf) 254:125042. https://doi.org/10.1016/j.polymer.2022.125042

Hines L, Petersen K, Lum GZ, Sitti M (2017) Soft actuators for small-scale robotics. Adv Mater 29(43):1603483. https://doi.org/10.1002/adma.201603483

Huang X, Wen W, Yang S, Sheng P (2006) Mechanisms of the giant electrorheological effect. Solid State Commun 139:581–588. https://doi.org/10.1016/j.ssc.2006.04.042

Jang HS, Kwon SH, Lee JH, Choi HJ (2019) Facile fabrication of core-shell typed silica/poly(diphenylamine)

composite microparticles and their electro-response. Polymer (Guildf) 182:121851(9). https://doi.org/10.1016/j.polymer.2019.121851

Jin E, Guo J, Yang F et al (2016) On the polymorphic and morphological changes of cellulose nanocrystals (CNC-I) upon mercerization and conversion to CNC-II. Carbohydr Polym 143:327–335. https://doi.org/10.1016/j.carbpol.2016.01.048

Kassab Z, Abdellaoui Y, Salim MH et al (2020) Micro- and nano-celluloses derived from hemp stalks and their effect as polymer reinforcing materials. Carbohydr Polym 245:116506. https://doi.org/10.1016/j.carbpol.2020.116506

Ko YG, Shin SS, Choi US et al (2011) Gelation of chitin and chitosan dispersed suspensions under electric field: effect of degree of deacetylation. ACS Appl Mater Interfaces 3:1289–1298. https://doi.org/10.1021/am200091r

Kolekar S, Venkatesh K, Oh JS, Choi SB (2019) Vibration controllability of sandwich structures with smart materials of electrorheological fluids and magnetorheological materials: a review. J Vib Eng Technol 7:359–377. https://doi.org/10.1007/s42417-019-00120-5

Kovaleva VV, Kuznetsov NM, Vdovichenko AY et al (2022a) Effect of temperature on the electrorheological behavior of porous chitosan particles in polydimethylsiloxane. Dokl Phys Chem 502:23–27. https://doi.org/10.1134/S0012501622020026

Kovaleva VV, Kuznetsov NM, Istomina AP et al (2022b) Low-filled suspensions of α-chitin nanorods for electrorheological applications. Carbohydr Polym 277:118792. https://doi.org/10.1016/j.carbpol.2021.118792

Kraev AS, Davydova OI, Nefedova TA et al (2007) Sol-Gel synthesis of titanium dioxide and titanium dioxide-hydroxypropyl cellulose hybrid material and electrorheological characteristics of their dispersions in poly(dimethylsiloxane). Colloid J 69:620–626. https://doi.org/10.1134/S1061933X07050122

Kuznetsov NM, Bakirov AV, Banin EP et al (2021a) In situ X-ray analysis of montmorillonite suspensions in polydimethylsiloxane: Orientation in shear and electric field. Colloids Surfaces A Physicochem Eng Asp 622:126663. https://doi.org/10.1016/j.colsurfa.2021.126663

Kuznetsov NM, Kovaleva VV, Zagoskin YD et al (2021b) Specific features of the porous polymeric particle composites application as fillers for electrorheological fluids. Nanobiotechnol Rep 16:840–846. https://doi.org/10.1134/S2635167621060148

Kuznetsov NM, Zagoskin YD, Bakirov AV et al (2021c) Is chitosan the promising candidate for filler in nature-friendly electrorheological fluids? ACS Sustain Chem Eng 9:3802–3810. https://doi.org/10.1021/acssuschemeng.0c08793

Kuznetsov NM, Zagoskin YD, Vdovichenko AY et al (2021d) Enhanced electrorheological activity of porous chitosan particles. Carbohydr Polym 256:117530. https://doi.org/10.1016/j.carbpol.2020.117530

Kuznetsov NM, Kovaleva VV, Belousov SI, Chvalun SN (2022a) Electrorheological fluids: from historical retrospective to recent trends. Mater Today Chem 26:101066. https://doi.org/10.1016/j.mtchem.2022.101066

Kuznetsov NM, Kovaleva VV, Volkov DA et al (2022b) Porous chitosan particles doped by in situ formed silver nanoparticles: electrorheological response in silicon oil. Polym Adv Technol 33:3643–3657. https://doi.org/10.1002/pat.5817

Kuznetsov NM, Vdovichenko AY, Bakirov AV et al (2022c) The size effect of faceted detonation nanodiamond particles on electrorheological behavior of suspensions in mineral oil. Diam Relat Mater 125:108967. https://doi.org/10.1016/j.diamond.2022.108967

Kuznetsov NM, Kovaleva VV, Vdovichenko AY, Chvalun SN (2023) Natural electrorheological fluids based on cellulose particles in olive oil: the filler size effect. Collod J 85:408–417

Lee HJ, Cho Y, Kang SW (2022) Low-cost process to utilize sodium salts for porous cellulose materials. J Ind Eng Chem 113:368–372. https://doi.org/10.1016/j.jiec.2022.06.011

León A, Reuquen P, Garín C et al (2017) FTIR and Raman characterization of TiO2 Nanoparticles coated with polyethylene glycol as carrier for 2-methoxyestradiol. Appl Sci 7:49. https://doi.org/10.3390/app7010049

Lim GH, Choi HJ (2017) Fabrication of self-assembled polyaniline tubes and their electrorheological characteristics. Colloids Surf A Physicochem Eng Asp 530:227–234. https://doi.org/10.1016/j.colsurfa.2017.07.063

Liu Z, Chen P, Jin X et al (2018) Enhanced electrorheological response of cellulose: a double effect of modification by urea-terminated silane. Polymers (Basel) 10:15–17. https://doi.org/10.3390/polym10080867

Malkin AY, Isayev AI (2005) Rheology: Concepts, methods, and applications. ChemTec Publishing, Toronto

Melikoğlu AY, Bilek SE, Cesur S (2019) Optimum alkaline treatment parameters for the extraction of cellulose and production of cellulose nanocrystals from apple pomace. Carbohydr Polym 215:330–337. https://doi.org/10.1016/j.carbpol.2019.03.103

Misono Y, Negita K (2004) Shear-induced particle rotation and its effect on electrorheological and dielectric properties in cellulose suspension. Phys Rev E 70:061412(6). https://doi.org/10.1103/PhysRevE.70.061412

Nasseri R, Deutschman CP, Han L et al (2020) Cellulose nanocrystals in smart and stimuli-responsive materials: a review. Mater Today Adv 5:100055. https://doi.org/10.1016/j.mtadv.2020.100055

Park S, Baker JO, Himmel ME et al (2010) Cellulose crystallinity index: measurement techniques and their impact on interpreting cellulase performance. Biotechnol Biofuels 3:10. https://doi.org/10.1186/1754-6834-3-10

Plachý T, Žitka J, Mrlík M et al (2021) Electrorheology of polyindole. Polymer (Guildf) 217:123448. https://doi.org/10.1016/j.polymer.2021.123448

See H (2000) Constitutive equation for electrorheological fluids based on the chain model. J Phys D Appl Phys 33:1625–1633. https://doi.org/10.1088/0022-3727/33/13/311

Seo YP, Choi HJ, Seo Y (2017) Analysis of the static yield stress for giant electrorheological fluids. Korea Aust Rheol J 29:215–218. https://doi.org/10.1007/s13367-017-0022-2

Sheng P, Wen W (2012) Electrorheological fluids: mechanisms, dynamics, and microfluidics applications. Annu Rev Fluid Mech 44:143–174. https://doi.org/10.1146/annurev-fluid-120710-101024

Sim B, Bae DH, Choi HJ et al (2016) Fabrication and stimuli response of rice husk-based microcrystalline

cellulose particle suspension under electric fields. Cellulose 23:185–197. https://doi.org/10.1007/s10570-015-0836-3

Sokolov MA, Kuznetsov NM, Belousov SI, Chvalun SN (2021) Effect of the dispersion medium viscosity on the electrorheological behavior of halloysite suspensions in polydimethylsiloxane. ChemChemTech 64:79–85. https://doi.org/10.6060/ivkkt.20216411.6402

Spence KL, Venditti RA, Habibi Y et al (2010) Bioresource technology the effect of chemical composition on microfibrillar cellulose films from wood pulps : mechanical processing and physical properties. Bioresour Technol 101:5961–5968. https://doi.org/10.1016/j.biortech.2010.02.104

Tilki T, Yavuz M, Karabacak C et al (2010) Investigation of electrorheological properties of biodegradable modified cellulose / corn oil suspensions. Carbohydr Res 345:672–679. https://doi.org/10.1016/j.carres.2009.12.025

Wolf MP, Salieb-Beugelaar GB, Hunziker P (2018) PDMS with designer functionalities—properties, modifications strategies, and applications. Prog Polym Sci 83:97–134. https://doi.org/10.1016/j.progpolymsci.2018.06.001

Wu J, Zhang L, Xin X et al (2018) The electrorheological fluids with high shear stress based on wrinkly tin titanyl oxalate. ACS Appl Mater Interfaces 10:6785–6792. https://doi.org/10.1021/acsami.8b00869

Wu J, Du X, Yin Z et al (2019) Preparation and characterization of cellulose nanofibrils from coconut coir fibers and their reinforcements in biodegradable composite films. Carbohydr Polym 211:49–56. https://doi.org/10.1016/j.carbpol.2019.01.093

Yarysheva AY, Bagrov DV, Bakirov VAV et al (2017) Polyethylene–Poly(ethylene oxide) hybrid films obtained by crazing and their structural peculiarities. Macromolecules 50:2881–2888. https://doi.org/10.1021/acs.macromol.6b02512

Yin J, Xia X, Xiang L et al (2009) The electrorheological effect of polyaniline nanofiber, nanoparticle and microparticle suspensions. Smart Mater Struct 18. https://doi.org/10.1088/0964-1726/18/9/095007

Yoon DJ, Kim YD (2006) Synthesis and electrorheological behavior of sterically stabilized polypyrrole-silica-methylcellulose nanocomposite suspension. J Colloid Interface Sci 303:573–578. https://doi.org/10.1016/j.jcis.2006.07.051

Zhang H, Luan Q, Li Y et al (2022) Fabrication of highly porous, functional cellulose-based microspheres for potential enzyme carriers. Int J Biol Macromol 199:61–68. https://doi.org/10.1016/j.ijbiomac.2021.12.069

Zhao Y, Moser C, Lindström ME et al (2017) Cellulose nanofibers from softwood, hardwood, and tunicate: preparation-structure-film performance interrelation. ACS Appl Mater Interfaces 9:13508–13519. https://doi.org/10.1021/acsami.7b01738